Synthesis and Characterization of Bismuth Oxide Nanoparticle by Thermal Decomposition of Bismuth-Based MOF and Evaluation of Its Nanocomposite

Motakef Kazemi, Negar*+; Rashidian, Morvarid
Department of Medical Nanotechnology, Faculty of Advanced Sciences and Technology, Tehran Medical Sciences, Islamic Azad University, Tehran, I.R. IRAN

Taghizadeh Dabbagh, Sima
Institute for Advanced Medical Technologies, Tehran University of Medical Sciences, Tehran, I.R. IRAN

Yaqoubi, Masoumeh
Department of Nanochemistry, Faculty of Pharmaceutical Chemistry, Tehran Medical Sciences, Islamic Azad University, Tehran, I.R. IRAN

ABSTRACT: *Metal-Organic Frameworks (MOFs) are an important class of highly porous hybrid materials. A bismuth-based MOF was prepared under solvothermal conditions via the self-assembly of primary building blocks at 100 °C for 3 h. Bismuth oxide nanoparticles (Bi_2O_3 NPs) were prepared by calcination and thermal decomposition of a bismuth-based MOF at 550 °C for 5 h for the first time. The nanocomposite was prepared by poly (methyl methacrylate) (PMMA) as a polymer matrix and bismuth oxide NPs as fillers. The bismuth oxide nanoparticles were characterized by Fourier Transform InfraRed (FT-IR) for determination of functional groups, X-Ray powder Diffraction (XRD) for evaluation of crystal structure, Dynamic Light Scattering (DLS) for investigation of size and size distribution, Scanning Electron Microscope (SEM) for the presentation of morphology and size, and Energy-Dispersive X-ray Spectroscopy (EDS) for determination of chemical composition. Based on the results, the bismuth oxide nanoparticles were observed with spherical morphology and the particle size of 60 nm. The bismuth oxide nanocomposites were evaluated by X-ray dosimeter test in comparison to lead and aluminum and air adsorbents for X-ray shielding, Diffuse Reflection Spectroscopy (DRS) for UltraViolet (UV) blocking, and antibacterial activity against Salmonella bacterial. Based on the results, the X-ray shielding is 31.9% compared with the lead with a thickness of 0.25 mm and 81.53% compared with aluminum with a thickness of 3 mm for the bismuth oxide nanocomposite. This nanocomposite has 70% UV blocking with antibacterial activity and it can have a good potential for biomedical and industrial applications.*

KEYWORDS: *Bismuth; Nanoparticle; Metal-organic framework; Nanocomposite.*

** To whom correspondence should be addressed.*
+ E-mail: motakef@iaups.ac.ir
1021-9986/2021/1/11-19 *9/$/5.09*

INTRODUCTION

The metal-organic framework is a new class of coordination polymers as porous organic-inorganic crystalline-hybrid compounds [1]. Recently, MOF has attracted much attention due to extensive design and synthesis [2], unique properties [3], and emerging applications [4]. MOFs have been studied extensively because of the presence of organic and inorganic sections, large surface area, high pore volume [5], and adjustable shape and pore [6]. These porous compounds are synthesized via an *in situ* self-assembly method from the coordination of polydentate ligands and metal ions (or metal clusters) with the expansion of porous network structures by different methods. Two common methods of MOF synthesis are the solvothermal [7] and solution [8-9] approach. The development of MOF synthesis has been playing a major role in the advancement of this field [10-12]. The bismuth-based MOF is one of the metal-organic coordination polymers with interesting properties [13-15]. The bismuth-based MOFs have created beneficial advantages such as semiconductor, photocatalysis, adsorbent, geometrically flexible, and abundant material with low toxicity for MOF construction [16-17].

The different methods have expanded for bismuth nanostructures synthesis with tunable size and shape parameters. The common methods of bismuth nanostructures synthesis include solution [18-19], solution combustion [20], solvothermal [21], hydrothermal [22], laser ablation [23], green synthesis [24], sol-gel [25], flame spray pyrolysis [26], and thermal decomposition [27-29]. Recently, nanomaterials have been prepared by thermal decomposition of metal-organic frameworks as new precursors, such as Cu nanoparticles from the $[Cu_3(btc)_2]$[btc = benzene-1,3,5-tricarboxylate) MOF [30], ZnO nanoparticles from $Zn_4O(1,4\text{-bdc})_3$ (MOF-5) [31], ZnO nanoparticles from $Zn_2(NDC)_2(DMF)_2.(H_2O)_4$ [H_2NDC = 2,6-naphthalene dicarboxylic acid and DMF = N,N'-dimethylformamide] [32], and PdO nanoparticles from a Pd(II)-based MOF [ligand = tetra-pyridyl porphyrin] [33]. The importance of bismuth nanoparticle is increased due to the main applications such as radiation protection [34-35], medicine [36], imaging and radiotherapy [23, 37], ion-selective electrode [38], optical and plasmonic properties [39-40], UV-Visible absorption [41], antibacterial activity [42], catalytic properties [19], and photocatalytic uses [43].

Radiology is responsible for significant medical advancements without risks. Medical application of X-rays offer a great benefit to patients. The amount of radiation doses has a significant increase of effectiveness in radiological protection using justification and optimization of diagnostic medical exposures. High doses of X-ray radiation have been caused to increase the risk for each individual. So, it is necessary that used personal protective equipment such as lead aprons, thyroid shields, and lead glasses during X-ray fluoroscopy. Lead is a good candidate for an X-ray shield due to its high density and high atomic number, but it is caused many discomforts because of disadvantages such as high weight and very toxic to the environment [44-45]. Bismuth nanostructures are important as a good candidate for radiation protection techniques with properties such as environmentally friendly, non-toxic, lead-free, and less weight compared to conventional lead-based shields [34, 46]. The modified polydimethylsiloxane nanocomposite with bismuth oxide was studied by *Yeow* and *coworkers* as shielding against diagnostic X-rays [47]. The polyimide/Bi_2O_3 composite was evaluated by Cherkashina and coworkers as for shielding of gamma (γ) radiation [48]. Poly (methyl methacrylate) has many advantages including low cost, biocompatibility, ease of processing, high resistance to UV light and weathering, excellent visible light transmission, unlimited coloring options, stability in the oral environment, acceptable aesthetics, and good processing ability. Several studies have been conducted with the goal of preparation of PMMA nanocomposite by using various methods for different applications [49]. Hence, one of the purpose is X-ray shielding of modified PMMA nanocomposite with Bi_2O_3 NPs.

Ultraviolet light is non-ionizing radiation in the electromagnetic spectrum including three regions UV-A (320–400 nm), UV-B (280-320 nm), and UV-C (180-280 nm). The earth's atmosphere shields the more harmful UV-C and the greater than 99% of UV-B radiation. The UV-A blocking is very important to prevention from the risk of exposure to direct sunlight [50]. The UV-absorber was introduced as one of the important applications of bismuth oxide [51]. Nanomaterial has been interesting for the UV blocking ability because of its small size and large surface area to volume ratio. Zinc oxide nanoparticles [52] and ZnO composite nanofibers [53] were reported in the UV blocking. Therefore, it is important to investigate the UV

blocking properties of modified PMMA nanocomposite with Bi_2O_3 NPs as another objective of this study. The antibacterial activity of nanostructures has been expanded due to the presence of metal, metal oxides, and organic materials [54]. Bismuth oxide nanoparticles can be developed to antibacterial activity against some pathogenic Gram-negative bacteria [55]. As a result, antibacterial activity is another goal of this study for modified PMMA nanocomposite with Bi_2O_3 NPs. In this work, bismuth oxide nanoparticles were prepared by thermal decomposition of bismuth-based MOF for the first time. The objective of the present study was to develop the modified PMMA nanocomposite with Bi_2O_3 NPs for X-ray shielding, UV blocking, and antibacterial activity.

EXPERIMENTAL SECTION

Materials

All chemicals used were analytical grade. Materials including bismuth nitrate ($Bi(NO_3)_3$), benzene 1,4-dicarboxylic acid (BDC), dimethylformamide (DMF), sodium hydroxide (NaOH), poly (methyl methacrylate) (PMMA), and dichloromethane (CH_2Cl_2) were purchased from Merck (Darmstadt, Germany).

Methods

Preparation of nanostructures

For the preparation of bismuth-based MOF, 0.145 g (0.3 mmol) bismuth nitrate was solved in 2.5 mL DMF, and 0.024 g (0.6 mmol) sodium hydroxide was added to the resulting solution. Then, 0.249 g (1.5 mmol) BDC was solved in 2.5 mL DMF, and the resulting solution was slowly added to the solution including metal centers. The mixture was sealed and stirred at 100 °C for 3 h [13]. The reaction mixture was cooled to room temperature and filtered. Then, the crystals were washed several times with DMF, and dried in the air. The thermal decomposition of a bismuth-based MOF was used to prepare α-Bi_2O_3 at 550 °C [56] in a furnace and static atmosphere of air for 5 h [57]. For the preparation of nanocomposite, different percentages of bismuth oxide nanoparticles were instigated and a suitable percentage was selected based on X-ray shielding. PMMA aqueous solution was prepared by dissolving in dichloromethane, and 70% bismuth nanoparticle was added to the solution under sonicate for 1 h. Then, the mixture was cast onto a Teflon plate and dried at room temperature.

Characterization

The samples were characterized by Fourier transform infrared, X-ray powder diffraction, dynamic light scattering, scanning electron microscope, energy-dispersive X-ray spectroscopy, X-ray shielding, UV blocking, and antibacterial activity. Fourier transform infrared spectrum was recorded on a Unicam Matson 1000 FT-IR spectrophotometer using a KBr disk at room temperature. Powder X-ray diffraction pattern was performed for evaluation of the crystalline structure of bismuth oxide NP using a Philips Company X'pert diffractometer utilizing Cu-Ka radiation (ASENWARE, AW-XBN300, China). Dynamic light scattering was reported size and size distribution of bismuth oxide nanoparticle (ZEN314, England). A scanning electron microscope has investigated the morphology and size of bismuth oxide NP (KYKY, EM3200, China). In this method, bismuth oxide nanoparticles were first coated by sputtering with a thin layer of gold and then studied by SEM. Energy-dispersive X-ray spectroscopy was evaluated the elemental and chemical analysis of bismuth oxide NP (ASK SEM-CL View VIS, Oxford Instruments, UK). X-ray absorption was used for X-ray shielding of nanocomposite (Giger-mini monitor, USA). Diffuse reflection spectroscopy was investigated for light absorption and UV blocking properties of nanocomposite (UV2550, Shimadzu). The antibacterial activity was evaluated using the disk diffusion method against *Salmonella* Gram-negative bacteria, strains ATCC 1231, procured from Islamic Azad University for bismuth oxide nanoparticle and nanocomposite. Müller-Hinton agar was used for antibacterial tests according to the Merck manufacturer's agenda. The inhibition zone was detected by the appearance of the agar.

RESULTS AND DISCUSSION

Fourier transform infrared spectroscopy

The FTIR absorption spectrum of the bismuth nanoparticle was recorded in the range of 400–4000 cm^{-1} (Fig. 1). The O–H stretching vibrations appear at 3421 cm^{-1}. The peak at 1400 cm^{-1} is related to C-O vibrations due to organic solvent. The peak at 435~505 cm^{-1} is originated from the metal-oxygen (Bi-O) bond. Fourier transform infrared results confirm the previous report [58].

X-ray diffraction

X-ray diffraction measurement was used to determine the crystalline structure of bismuth nanoparticle in 2θ

range 20 to 60° after decomposition at 550°C (Fig. 2). The sharp peak was observed at 2θ around 28°, and all diffraction peaks can be indexed the monoclinic α-Bi_2O_3 (JCPDS card No. 41-1449). Based on the XRD results, characteristic peaks of nanoparticles were corresponding with the crystalline structure α-Bi_2O_3 as the most thermodynamically stable phase. This result is similar to the patterns of previously reported papers by other researchers [59].

Dynamic light scattering

The size and distribution diagram of the bismuth nanoparticle was determined by dynamic light scattering (Fig. 3). DLS result showed a single-peak with a size of about 70 nm and a narrow distribution at room temperature.

Scanning electron microscope

Morphology and size of bismuth oxide nanoparticles were characterized by a scanning electron microscope (Fig. 4). The SEM image demonstrated the nanoparticles with spherical morphology. The particle size was estimated to be 60 nm, and confirmed the DLS result.

Energy-dispersive X-ray spectroscopy

Energy-dispersive X-ray spectroscopy was used to evaluate the chemical composition of bismuth oxide nanoparticles. This analysis was clearly showed the identification of strong peaks of bismuth (Bi) and oxygen (O) elements. The EDS analysis of bismuth oxide NP exhibited absorption bands with peaks at 2.4, 3.2, 10.8, and 11.8 keV, which illustrated a typical absorption of the metallic bismuth. The energy-dispersive X-ray spectroscopy result is similar to a previous report [58].

X-ray shielding

The X-ray shielding was evaluated using radiation dosimetry by nanocomposite. Bismuth is a good substitute compared with lead because it has a higher atomic number (83 instead of 82) and less density (9.78 g/cm^3 instead of 11.34 g/cm^3) with less toxicity. X-ray intensity was examined at 40, 50, 60 kV, and 0.1 mAh, and compared with air, aluminum 2.5 and 3 mm, and lead 0.25 mm (Table 1).

Based on the results, the ability to X-ray absorb of nanocomposite is similar to 99% aluminum with a thickness of 3 mm in 40 and 50 kV, and it is similar to 99%

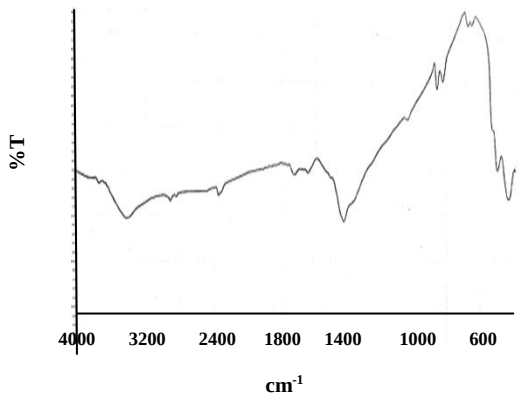

Fig. 1: FT-IR bismuth oxide nanoparticle.

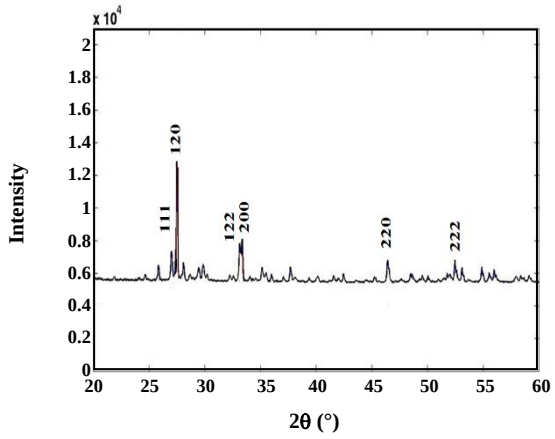

Fig. 2: XRD bismuth oxide nanoparticle.

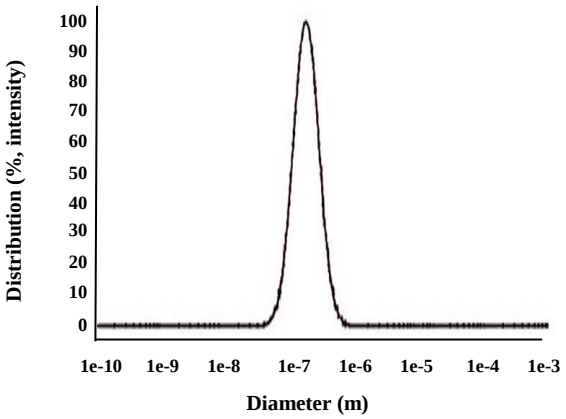

Fig. 3: DLS bismuth oxide nanoparticle.

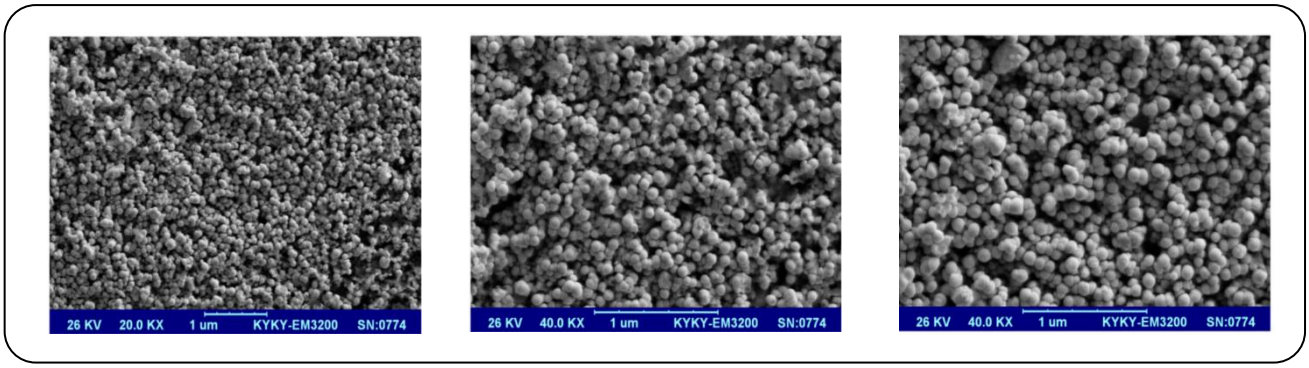

Fig. 4: SEM bismuth oxide nanoparticle.

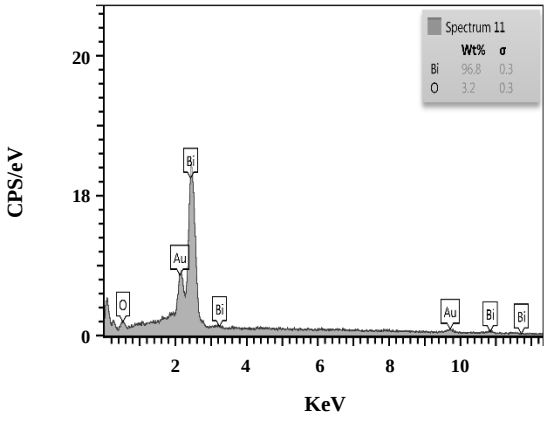

Fig. 5: EDS bismuth oxide nanoparticle.

aluminum with a thickness of 2.5 mm by increasing to 60 kV. In 60 kV, the absorption percentage of nanocomposite is 31.9% compared with the lead with a thickness of 0.25 mm and 81.53% compared with aluminum with a thickness of 3 mm. The result is based on the previous report for modified polydimethylsiloxane nanocomposite with bismuth oxide nanopowder at a tube potential of 60 kV in comparing to 0.25 mm lead sheet [47]. Therefore, bismuth oxide nanocomposite is a good candidate as X-ray shielding for the research development of radiation protection.

Diffuse reflection spectroscopy

The DRS absorption spectra of bismuth oxide nanoparticle and its nanocomposite showed the ultraviolet protective properties in three Ultraviolet: UV-A, UV-B, and UV-C (Fig. 6). UV blocking properties of bismuth oxide nanocomposite were investigated for the first time. Based on DRS spectra, the absorption peak observed in range of 200-400 nm that approved UV blocking property. the absorption percentages of ultraviolet radiation were observed 90% for bismuth oxide nanoparticle and 70% for its nanocomposite. Based on the result, UV blocking is due to the presence of bismuth oxide nanoparticles. The results confirm the previous report about UV blocking of [60] and modified Poly-o-phenylenediamine nanocomposite with TiO_2 nanoparticles [61]. In nanocomposite, the presence of PMMA polymer was caused by the reduction of UV blocking and the increase of visible barrier.

Antibacterial test

The antibacterial activity was measured against *Salmonella* as Gram-negative bacteria by disk diffusion method for nanocomposite and bismuth oxide nanoparticle with concentration 0.01 g/ml. The zone inhibition was examined approximately 8.6 mm and the same for bismuth oxide nanoparticle and nanocomposite. Based on the result, similar antibacterial activity is due to the high percentage of bismuth oxide nanoparticles in nanocomposite. In Gram-negative bacterium, the cell wall is composed of a thin layer of peptidoglycan surrounded by a membranous structure called the outer membrane. The presence of carboxylic groups causes the negative charge of bacterial cells at biological pH. The main mechanisms of antibacterial activity are electrostatic forces and adhesion of the opposite charges of Gram-negative bacterium and bismuth oxide nanoparticle. Bismuth oxide nanoparticles can react with proteins and result in the inactivation of protein molecules and vital enzymes. The results approved the previous report about the antibacterial properties of bismuth oxide aqueous colloidal nanoparticles [62]. Therefore, bismuth oxide nanoparticles and its nanocomposite are good candidates as antibacterial agents for research development.

Table 1: X-ray shielding nanocomposite.

mAh	kV	air	Bi_2O_3	Al 2.5mm	Al 3mm	Pb 0.25 mm
0.1	40	4.68	2.55	2.64	2.11	0.21
0.1	50	5.96	4.23	4.12	3.89	1.89
0.1	60	8.61	6.32	6.47	7.02	2.75

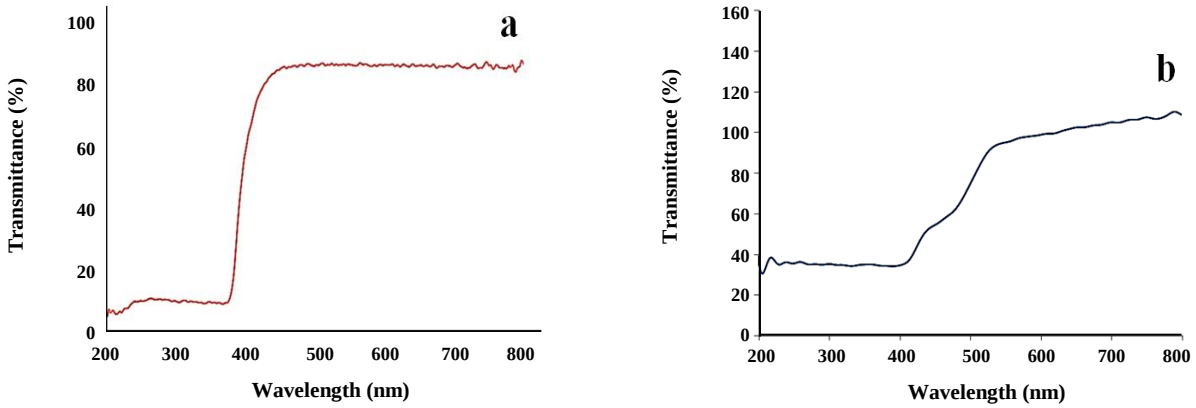

Fig. 6: DRS of (a) bismuth oxide nanoparticle and (b) its nanocomposite.

CONCLUSIONS

The bismuth oxide nanoparticle was synthesized by thermal decomposition of bismuth-based MOF for the first time. DLS results emphasized the formation of nanoparticles with narrow distribution and the particle size was nanometre. Based on SEM result, nanoparticles were observed with spherical morphology and size of 60 nm. In the present study, we successfully modified PMMA nanocomposite with bismuth oxide NP for X-ray shielding, UV blocking, and antibacterial activity applications. These properties can result in many advantages in the future with less harm and toxicity to human health and more safety compared to lead as a protective material.

Received : Jul. 26, 2020 ; Accepted : Nov. 3, 2020

REFERENCES

[1] Rowsell J.L.C., Yaghi O.M., Metal-Organic Frameworks: A New Class of Porous Materials, *Micropor Mesopor Mat*., **73**: 3–14 (2004).

[2] Li H., Eddaoudi M., O'Keeffe M., Yaghi O., Design and synthesis of an Exceptionally Stable and Highly Porous Metal-Organic Framework, *Nature*., **402**: 276–279 (1999).

[3] Khan N.A., Hasan Z., Jhung S.H., Beyond Pristine Metal-Organic Frameworks: Preparation and Application of Nanostructured, Nanosized, and Analogous MOFs, *Coord. Chem. Rev*., **376**: 20–45 (2018).

[4] Czaja A.U., Trukhan N., Muller U., Industrial Applications of Metal-Organic Frameworks, *Chem. Soc. Rev*., **38**: 1284–1293 (2009).

[5] Sosa J.D., Bennett T.F., Nelms K.J., Liu B.M., Tovar R.C., Liu Y., Metal-Organic Framework Hybrid Materials and Their Applications, *Crystals*., **8**: 325-348 (2018).

[6] Chen B., Xiang S., Qian G., Metal−organic Frameworks with Functional Pores for Recognition of Small Molecules, *Acc. Chem. Res*., **43(8)**: 1115-1124 (2010).

[7] Motakef-Kazemi N., Shojaosadati S.A., Morsali A., Evaluation of the Effect of Nanoporous Nanorods $Zn_2(bdc)_2(dabco)$ Dimension on Ibuprofen Loading and Release, *JICS*., **13(7)**: 1205-1212 (2016).

[8] Motakef-Kazemi, N., Shojaosadati, S.A., Morsali, A., *In Situ* Synthesis of a Drug-Loaded MOF at Room Temperature, *Micropor Mesopor Mat*., **186**: 73-79 (2014).

[9] Tranchemontagne D.J., Hunt J.R., Yaghi O.M., Room Temperature Synthesis of Metal-Organic Frameworks: MOF-5, MOF-74**,** MOF-177, MOF-199, and IRMOF-0, *Tetrahedron*., **64**: 8553–8557 (2008).

[10] Zhou H.C., Long J.R., Yagh, O.M., Introduction to Metal–Organic Frameworks, *Chem Rev*., **112(2)**: 673–674 (2012).

[11] Yuan S., Feng L., Wang K., Pang J., Bosch M., Lollar C., Sun Y., Qin J., Yang X., Zhang P., Wang Q., Zou L., Zhang Y., Zhang L., Fang Y., Li J., Zhou H.C., Stable Metal-Organic Frameworks: Design, Synthesis, and Applications. *Adv Mater*., **30(37)**: 1704303 (2018).

[12] Mehmandous M.R., Motakef-Kazemi N., Ashouri F., Nitrate Adsorption from Aqueous Solution by Metal–Organic Framework MOF-5, *IJSTS*., 1-7 **43(2)**: 443–449 (2019).

[13] Thirumurugan A., Cheetham A.K., Anionic Metal-Organic Frameworks of Bismuth Benzenedicarboxylates: Synthesis, Structure and Ligand-Sensitized Photoluminescence, *Eur. J. Inorg. Chem*., **2010(24)**: 3823–3828 (2010).

[14] Savage M., Yang S., Suyetin M., Bichoutskaia E., Lewis W., Blake A.J., Barnett S.A., Schrçder M., A Novel Bismuth-Based Metal-Organic Framework for High Volumetric Methane and Carbon Dioxide Adsorption. *Chem. Eur. J*., **20**: 8024–8029 (2014).

[15] Ataei F., Dorranian D., Motakef-Kazemi, N., Bismuth-Based Metal-Organic Framework Prepared by Pulsed Laser Ablation Method In Liquid, *J. Theor. Appl. Phys*., **14**:1–8 (2020).

[16] Wang G., Sun Q., Liu Y., Huang B., Dai Y., Zhang X., Qin X., A Bismuth-Based Metal-Organic Framework as an Efficient Visible-Light-Driven Photocatalyst, *Chem Eur J*., **21**: 2364–2367 (2015).

[17] Savage M., Yang S., Suyetin M., Bichoutskaia E., Lewis W., Blake A.J., Barnett S.A., Schrçder M., A Novel Bismuth- Based Metal-Organic Framework for High Volumetric Methane and Carbon Dioxide Adsorption, *Chem. Eur. J*., **20**: 1-14 (2014).

[18] Solanki, P.R., Singh, J., Rupavali, B., Tiwari, S., Malhotr, B.D., Bismuth Oxide Nanorods Based Immunosensor for Mycotoxin Detection, *Mater. Sci. Eng. C*., **70**: 564–571 (2017).

[19] Xia F., Xu X., Li X., Zhang L., Zhang L., Qiu H., Wang W., Liu Y., Gao J., Preparation of Bismuth Nanoparticles in Aqueous Solution and its Catalytic Performance for the Reduction of 4-Nitrophenol, *Ind. Eng. Chem. Res*., **53(26)**:10576–10582 (2014).

[20] La J., Huang Y., Luo G., Lai J., Liu C., Chu G., Synthesis of Bismuth Oxide Nanoparticles by Solution Combustion Method, *Particul. Sci. Technolo*., **31(3)**: 287-290 (2012).

[21] Wu, J., Qin, F., Lu, Z., Yang, H.J., Chen, R., Solvothermal Synthesis of Uniform Bismuth Nanospheres Using poly(N-vinyl-2-pyrrolidone) as a Reducing Agent. *Nanoscale Res. Lett*., **6(1)**: 66 (2011).

[22] Zulkifli, Z.A., Razak, K.A., Rahman, W.N.W.A., Abidin, S.Z., Synthesis and Characterisation of Bismuth Oxide Nanoparticles Using Hydrothermal Method: the Effect of Reactant Concentrations and Application in Radiotherapy, *JPCS*., **1082**: 012103 (2018).

[23] Torrisi L., Silipigni L., Restuccia N., Cuzzocrea S., Cutroneo M., Barreca F., Fazio B., Di Marco G., Guglielmino S., Laser-Generated Bismuth Nanoparticles for Applications in Imaging and Radiotherapy, *J. Phys. Chem. Solids*., **119**: 62-70 (2018).

[24] Nazari P., Faramarzi M.A., Sepehrizadeh Z., Mofid M.A., Bazaz R.D., Shahverdi A.R., Biosynthesis of Bismuth Nanoparticles Using Serratia Marcescens Isolated from the Caspian Sea and Their Characterization, *IET Nanobiotechnol*., **6(2)**: 58-62 (2012).

[25] Mallahi M., Shokuhfar A., Vaezi M.R., Esmaeilirad A., Mazinani V., Synthesis and Characterization of Bismuth Oxide Nanoparticles Via Sol-Gel Method *AJER*., **3(4)**: 162-165 (2014).

[26] Mädler, L., Pratsinis, S.E., Bismuth Oxide Nanoparticles by Flame Spray Pyrolysis, *J. Am. Ceram. Soc*., **5**(7): 1713–1718 (2004).

[27] Carotenuto, G., Hison, C.L., Capezzuto, F., Palomba, M., Synthesis and Thermoelectric Characterization of Bismuth Nanoparticles, *J. Nanopart. Res*., **11(7)**: 1729-1738 (2009).

[28] Schulz S., Heimann S., Wölper C., Assenmacher W., Synthesis of Bismuth Pseudo Cubes by Thermal Decomposition of Bi_2Et_4. *Chem Mater*., **24 (11)**: 2032–2039 (2012).

[29] Huang, Y.J., Zheng, Y.Q., Zhu, H.L., Wang, J.J. Hydrothermal Synthesis of Bismuth(III) Coordination Polymer and its Transformation to Nano α-Bi_2O_3 for Photocatalytic Degradation, *J. Solid. State. Chem*., **239**: 274-281 (2016).

[30] Chen L., Shen Y., Bai J., Wang C., Novel Symmetrical Coralloid Cu 3D Superstructures: Solid-State Synthesis from a Cu-Carboxylate MOF and Their in-situ Thermal conversion, *J. Solid State Chem*., **182**: 2298-2306 (2010).

[31] Zhang L., Hu Y.H., A systematic Investigation of Decomposition of Nano $Zn_4O(C_8H_4O_4)_3$ Metal−Organic Framework, *J. Phys. Chem. C*., **114(6)**: 2566-2572 (2010).

[32] Shahangi Shirazi F., Akhbari K., Preparation of Zinc Oxide Nanoparticles from Nanoporous Metal-Organic Framework with One-Dimensional Channels Occupied with Guest Water Molecules, *Inorganica Chimica Acta*., **436**: 1–6 (2015).

[33] Bagchi V., Bandyopadhyay D., *In situ* Generation of Palladium Oxide Nano-Crystals, *J. Organomet. Chem*., **694**: 1259-1262 (2009).

[34] Shirkhanloo H., Saffari M., Amini S.M., Rashidi M., Novel semisolid Design Based on Bismuth Oxide (Bi_2O_3) Nanoparticles for Radiation Protection. *Nanomed. Res. J*., **2(4)**: 230-238 (2017).

[35] Jiao L., Li G., Deng J., Su M., Nanocellulose Templated Growth of Ultra-Small Bismuth Nanoparticles for Enhanced Radiation Therapy, *Nanoscale*., **10(14)**: 6751-6757 (2018).

[36] Oviedo M.J., Contreras O.E., Rosenstein Y., Vazquez-Duhalt R., Macedo Z.S., Carbajal-Arizaga G.G., Hirata G.A., New Bismuth Germanate Oxide Nanoparticle Material for Biolabel Applications in Medicine, *J. Nanomater*., **2016**: 1-10 (2016).

[37] Yang C., Guo C., Guo W., Zhao X., Liu S., Han X., Multifunctional Bismuth Nanoparticles as Theranostic Agent for PA/CT Imaging and NIR Laser-Driven Photothermal Therapy, *ACS Appl Nano Mater*., **1(2)**: 820–830 (2018).

[38] Liu L., Wang L., Yin H., Li Y., He X., The Preparation and Application of Bismuth (III) Ion-Selective Electrode Based on Nanoparticles of Bismuth Sulfide, *Anal Lett*., **39(5)**: 879-890 (2007).

[39] Jarka P., Tanskia T., Matysiaka W., Krzeminskia L., Hajduk B., Bilewicz M., Manufacturing and investigation of Surface Morphology and Optical Properties of Composite Thin Films Reinforced by TiO2, Bi2O3 and SiO2 Nanoparticles, *Appl. Surf. Sci*., **424(2)**: 206-212 (2017).

[40] Tian Y., Toudert J., Nanobismuth: fabrication, Optical, and Plasmonic Properties-Emerging Applications, *J. Nanotechnol.*, **2018**: 1-23 (2018).

[41] Wang Y.W., Hong B.H., Kim K.S., Size Control of Semimetal Bismuth Nanoparticles and the UV−Visible and IR Absorption Spectra, *J. Phys. Chem. B*., **109**(15): 7067-7072 (2005).

[42] Vega-Jiménez A.L., Almaguer-Flores A., Flores-Castañeda M., Camps E., Uribe-Ramírez M., Aztatzi-Aguilar O.G., De Vizcaya-Ruiz A., Bismuth Subsalicylate Nanoparticles with Anaerobic Antibacterial Activity for Dental Applications, *Nanotechnology*., **28(43)**: 435101 (2017).

[43] Raza W., Haque M.M., Muneer M., Harada T., Matsumura M., Synthesis, Characterization and Photocatalytic Performance of Visible Light-Induced Bismuth Oxide Nanoparticle, *J Alloy Compd*., **648**: 641-650 (2015).

[44] Wall B.F., Kendall G.M., Edwards AA.., Bouffler S., Muirhead C.R., Meara J.R., What are the Risks from Medical X-Rays and other Low Dose Radiation? *Br. J. Radiol*., **79(940)**: 285-294 (2006).

[45] Hulbert S.M., Carlson K.A., Is Lead Dust within Nuclear Medicine Departments a Hazard to Pediatric Patients? *J. Nucl. Med. Technol*., **37(3)**: 170-172 (2009).

[46] Zhou P., Lv J., Xu H., Wang X., Sui X., Zhong Y., Wang B., Chen Z., Feng X., Zhang L., Mao Z., Functionalization of Cotton Fabric with Bismuth Oxyiodide Nanosheets: Applications for Photodegrading Organic Pollutants. UV Shielding and Self-Cleaning. *Cellulose*., **26(4)**: 2873–2884 (2019).

[47] Nambiar S., Osei E.K., Yeow J.T.W., Polymer Nanocomposite-Based Shielding Against Diagnostic X-Rays, *J. Appl. Polym. Sci*., **127(6)**: 4939-4946 (2012).

[48] Pavlenko V.I., Cherkashina N.I., Yastrebinsky R.N., Synthesis and Radiation Shielding Properties of Polyimide/Bi_2O_3 Composites, *Heliyon*., **5(5)**: e01703 (2019).

[49] Ali U., Abd Karim K.J.B., Aziah Buang N., A Review of the Properties and Applications of Poly (methyl methacrylate) (PMMA), *Polym. Rev*., **55(4)**: 678-705 (2015).

[50] Hajiashrafi S., Motakef-Kazemi N., Green Synthesis of Zinc Oxide Nanoparticles Using Parsley Extract, *Nanomed Res J*., **3(1)**: 44-50 (2018).

[51] Perez-Mezcua D., Sirera R., Jimenez R., Bretos I., Dobbelaere C.D., Hardy A., Van Bael M.K., Calzad M.L., A UV-Absorber Bismuth(III)-Nmethyldiethanolamine Complex as a Low-Temperature Precursor for Bismuth-Based Oxide Thin Films, *J. Mater. Chem. C*., **2**: 8750–8760 (2014).

[52] Becheri A., Durr M., Nostro P.L., Baglioni P., Synthesis and Characterization of Zinc Oxide Nanoparticles**:** Application to Textiles as UV-Absorbers, *J. Nanopart. Res*., **10**: 679–689 (2008).

[53] Im, Y.M., Oh, T.H., Nathanael, J.A., Jang, S.S., Effect of ZnO nanoparticles Morphology on UV Blocking of Poly (vinylalcohol)/ZnO Composite Nanofibers, *Mater Lett*., **147**: 20–24 (2015).

[54] Hossain F., Perales-Perez O.J., Hwang S., Roman F., Antimicrobial Nanomaterials as Water Disinfectant: Applications, Limitations and Future Perspectives, *Sci. Total. Environ*., **466-467**: 1047-1059 (2014).

[55] Jassim A.M.N., Farhan S.A., Salman J.A.S., Khalaf K.J., Al Marjani M.F., Mohammed M.T., Study the Antibacterial Effect of Bismuth Oxide and Tellurium Nanoparticles, *Int. J. Chem. Biol. Sci*., **1(3)**: 81-84 (2015).

[56] Salazar-Pérez A.J., Camacho-López M.A., Morales-Luckie R.A., Sánchez-Mendieta V., Ureña-Núñez F., Arenas-Alatorre J., Structural Evolution of Bi_2O_3 Prepared by Thermal Oxidation of Bismuth Bano-Particles, *Superf. Vacío*., **18(3)**: 4-8 (2005).

[57] Hajiashrafi S., Motakef-Kazemi N., Preparation and Evaluation of ZnO Nanoparticles by Thermal Decomposition of MOF-5. *Heliyon.*, **5**: e02152 (2019).

[58] Sood S., Umar A., Mehta S.K., Kansal S.K., α-Bi_2O_3 Nanorods: An Efficient Sunlight Active Photocatalyst for Degradation of Rhodamine B and 2,4,6-Trichlorophenol, *Ceram Int*., **41(3)**: 3355-3364 (2015).

[59] Gotić, M., Popović, S., Musić, S., Influence of Synthesis Procedure on The Morphology of Bismuth Oxide Particles, *Mater Lett*., **61**: 709–714 (2007).

[60] Maruthamani, D., Vadivel, S., Kumaravel, M., Saravanakumar, B., Paul, B., Dhar, S.S., Habibi-Yangjeh, A., Manikandan, A., Ramadoss, G., Fine cutting Edge Shaped Bi_2O_3rods/Reduced Graphene Oxide (RGO) Composite for Supercapacitor and Visible-Light Photocatalytic Applications, *J. Colloid Interface Sci*., **498**: 449-459 (2017).

[61] Yang C., Dong W., Cui G., Zhao Y., Shi X., Xia X., Tang B., Wang W., Highly-Efficient Photocatalytic Degradation of Methylene Blue by Popd-Modified TiO_2 Nanocomposites Due to Photosensitization-Synergetic Effect of TiO_2 with PoPD, *Sci. Rep*., **7**: 3973 (2017).

[62] Hernandez-Delgadillo R., Velasco-Arias D., Diaz D., Zumeta-Dube I., Arevalo-Niño K., Cabral-Romero C., Martinez-Sanmiguel, J.J., Bismuth oxide Aqueous Colloidal Nanoparticles Inhibit *Candida Albicans* Growth and Biofilm Formation, *Int. J. Nanomedicine*., **8**: 1645–1652 (2013).